

Counterion-only electrical double layers: An application of density functional theory

Longcheng Liu

Citation: *The Journal of Chemical Physics* **143**, 064902 (2015); doi: 10.1063/1.4928508

View online: <http://dx.doi.org/10.1063/1.4928508>

View Table of Contents: <http://scitation.aip.org/content/aip/journal/jcp/143/6?ver=pdfcov>

Published by the [AIP Publishing](#)

Articles you may be interested in

Properties of a planar electric double layer under extreme conditions investigated by classical density functional theory and Monte Carlo simulations

J. Chem. Phys. **141**, 064701 (2014); 10.1063/1.4892415

Electrical double layers and differential capacitance in molten salts from density functional theory

J. Chem. Phys. **141**, 054708 (2014); 10.1063/1.4891368

Structure of cylindrical electric double layers: A systematic study by Monte Carlo simulations and density functional theory

J. Chem. Phys. **129**, 154906 (2008); 10.1063/1.2992525

Molecular solvent model of cylindrical electric double layers: A systematic study by Monte Carlo simulations and density functional theory

J. Chem. Phys. **129**, 154707 (2008); 10.1063/1.2981057

Structure of spherical electric double layers: A density functional approach

J. Chem. Phys. **127**, 034502 (2007); 10.1063/1.2750335



NEW Special Topic Sections

NOW ONLINE
Lithium Niobate Properties and Applications:
Reviews of Emerging Trends

AIP | Applied Physics
Reviews

Counterion-only electrical double layers: An application of density functional theory

Longcheng Liu^{a)}

*Department of Chemical Engineering and Technology, Royal Institute of Technology,
S-100 44 Stockholm, Sweden*

(Received 22 April 2015; accepted 31 July 2015; published online 11 August 2015)

Within the framework of density functional theory, a self-consistent approach of weighted correlation approximation is developed to give an accurate account of the cross correlations between the Coulombic interaction and the hard-sphere exclusion in the counterion-only electrical double layers. Application of the approach to the cases of practical interest, against the Monte Carlo simulations, shows that it is excellent in describing the structural properties and the pressures of the confined solutions involving both mono- and divalent counterions between two planar charged walls. In particular, the study suggests that the relative importance of electrostatic correlations in comparison to the effects of ionic excluded volume and direct Coulomb interactions depends on the valency of the counterions and the surface charge density. In a clay system with mixed counterions, the competition between the mono- and divalent ions results in a large swelling when the fraction of surface charge compensated by monovalent counterions is greater than 30%. In the opposite situation involving mostly divalent counterions, a limited swelling is found and the attraction between the clay particles favors the formation of stacks incorporating a water layer of about 1.0 nm. These findings are consistent with experimental observations, giving insight into some mechanisms governing the stability of colloidal clay in salt-free or dilute solutions. © 2015 AIP Publishing LLC. [<http://dx.doi.org/10.1063/1.4928508>]

I. INTRODUCTION

Since the pioneer work of Evans and co-workers,^{1,2} different approaches of density functional theory (DFT) have been developed over the years to study the interfacial properties of electrical double layers (EDLs). These include the weighted-density approximation (WDA),^{3,4} the reference fluid density (RFD)^{5,6} approximation, and the weighted-correlation approximation (WCA),^{7,8} etc., in addition to the classical bulk-fluid perturbation approach,^{9–12} to DFT. Although different in one way or the other, they all try to apply the available knowledge from the mean spherical approximation (MSA)^{13,14} for a homogeneous charged hard-sphere fluid to approximate the structural properties of inhomogeneous EDLs. The objective is to give a faithful description of ion-ion correlations that are entirely neglected in the Poisson-Boltzmann equation¹⁵ or the modified Gouy-Chapman theory.^{16,17} As a result, these approaches have been shown to be successful to a great extent in describing those non-intuitive electrostatic phenomena associated with the EDLs of a system in equilibrium with a bulk electrolyte.^{3–12} None of them had, however, ever been applied to counterion-only systems in equilibrium with pure water. The reason for this is, perhaps, due to the lack of a sound knowledge or a good approximation of the chemical potentials of counterions involved in the canonical system under a variety of conditions.

Note worthily, in a counterion-only or salt-free EDL, the only ions present in the solution are counterions that originate from the solid-liquid interface, and there is not a salt reservoir of finite concentration that dissociates the electrolyte and thereby makes the chemical potential of the ionic species constant throughout the system.^{18,19} This fact stimulated the development of a constrained entropy maximization approach by Briscoe and Attard,¹⁹ in order to highlight the distinction between the different thermodynamic foundations upon which the counterion-only and the normal double layer theories are established. Moreira and Netz¹⁸ developed, within a field-theoretic framework, a strong-coupling theory for counterion distributions in the case of a planar charged wall. These achievements can all be regarded as an extension or complement of the Poisson-Boltzmann approach, because of the treatment of ions as individual point charges. By contrast, Kjellander *et al.*^{20,21} showed that the anisotropic hypernetted chain (HNC) approximation could well be applied in the integral equation theory to accurately account for the excluded volume effects due to the finite size of ions and for the electrostatic correlations in the counterion-only EDLs. A question then arises: Can the DFT approaches also be successful for description of EDL systems with only counterions present. This motivates us to develop a self-consistent WCA approach, still along the line of the reference-fluid perturbation method^{3–12} to DFT, trying to address the thermodynamic effect of the absence of a salt reservoir on the double layer interactions. The result would not only demonstrate the versatility of the DFT but also reveal the importance of a suitable construction of the reference fluid

^{a)}Electronic mail: lliu@ket.kth.se. Tel.: +46 8 790 6416. Fax: +46 8 10 52 28.

in evaluating the cross correlations between the Coulombic interaction and the hard-sphere exclusion.

More importantly, application of the self-consistent WCA approach will help us to better understand, e.g., the swelling properties of montmorillonite,²² and the erosion behavior of bentonite^{23–25} in salt-free or dilute solutions. When used to interpret experimental results,^{26,27} the prediction of the self-consistent WCA approach may also give insight into the mechanisms governing the formation and breakup of montmorillonite particles and the demixing effect of exchangeable cations on the stability²⁸ of bentonite colloids under different conditions.

To facilitate presentations and discussion, this contribution is structured as follows. In Section II, the model system and the Monte Carlo (MC) simulations are briefly described. In Section III, the self-consistent WCA approach is detailed within the framework of DFT. In Section IV, we discuss the performance of the self-consistent WCA approach in describing the pressure of counterion-only EDLs, with a focus on the divalent counterion dominated cases, and then interpret some of the experimental results. The summary and conclusions are given in Section V.

II. MODEL AND MONTE CARLO SIMULATIONS

The system of interest consists of a primitive model of electrolyte with common ionic diameter d between two infinitely large, planar hard walls. The ions, modeled as hard spheres with a point electric charge embedded at the centre, are composed only of mono- and divalent counterions that are dissolved in a solvent considered to be a uniform dielectric continuum with a relative dielectric constant ϵ_r . The walls have the same ϵ_r and have a structureless surface with a uniform surface charge density σ .

Given that the walls are located at $z = 0$ and $z = h + d$, respectively, the interaction potential between an ion i at z and the walls can be written as

$$v_i(z) = \begin{cases} \infty, & z > h + d/2, \\ -\frac{q_i \sigma (h + d)}{2\epsilon_0 \epsilon_r}, & d/2 \leq z \leq h + d/2, \\ \infty, & z < d/2, \end{cases} \quad (1)$$

where the separation of the walls, h , is taken as the distance between the points of closest approach of the ions to the wall surface, q_i is the charge of ion i , and ϵ_0 is the permittivity of the vacuum.

The pair potential of interaction between ions i and j , separated by a distance r , is given by

$$u_{ij}(r) = \begin{cases} \frac{q_i q_j}{4\pi \epsilon_0 \epsilon_r r}, & r \geq d, \\ \infty, & r < d. \end{cases} \quad (2)$$

As such, the primitive model does not account explicitly for the structuring of the solvent molecules and any image charge effects and it simply reduces the short-range interactions to be hard sphere interactions. This might limit its capability to give reliable results, but still it allows verification of theoretical predictions by molecular simulations.

Perhaps mainly for this reason, the primitive model has frequently been used in both theoretical studies and MC simulations.^{29,30}

Since, in the present study, no coions are included in the model system, the MC simulations can be performed in the canonical ensemble with the traditional Metropolis algorithm.³⁰ To be specific, we consider the simulation box as a rectangular prism with the dimensions $a \times a \times h$, where a is defined to be large enough to give a sufficient number of counterions in the box. The temperature T , the number N_i , and the ratio of mono- and divalent counterions in the system are fixed, and

$$\sum_i N_i q_i = -2\sigma a^2, \quad (3)$$

such that the model system is kept electrostatically neutral. Periodic boundary conditions in the lateral directions with the minimum image convention are applied, as it is usually done.^{20,21} The long-range electrostatic interactions due to counterions outside the simulation box are estimated with the method³¹ of infinite, continuously moving, charged sheets with each containing a square hole corresponding to the simulation box.

In the simulations, the total number of counterions in the simulation box is chosen to be greater than 150 (to check the convergence of the MC simulations with the number of counterions, systems with twice as many particles have been tested and no significant differences have been observed). For all cases, 200 000 configurations per particle are generated to equilibrate the system, and at least 600 000 configurations per particle are applied to calculate the density profile of each kind of counterions against the planar charged walls. The contact values are calculated by extrapolation of the logarithm of the density profiles to the contact distance,³² and they are used to evaluate the pressure of the confined solution (without accounting for the van der Waals interaction¹⁵ between the walls) by^{20,21}

$$P = k_B T \sum_i \rho_i(d/2) - \frac{\sigma^2}{2\epsilon_0 \epsilon_r}, \quad (4)$$

where k_B is the Boltzmann's constant, $\rho_i(d/2)$ is the number density of the counterion species i at the point of closest approach to the planar charged wall, and the summation runs over the two kind of counterions involved in the system.

III. SELF-CONSISTENT APPROACH OF WEIGHTED CORRELATION APPROXIMATION

For the system under consideration, the inhomogeneity in density distribution $\rho_i(z)$ is a consequence of the external potential, $v_i(z)$, due to the infinitely large, charged, planar hard walls. At equilibrium, the chemical potential that can be thought of as a quantitative measure of the tendency of an ion to escape from the confined solution must be constant throughout the entire system, and it can be written for each ionic species as^{9,10}

$$\mu_i = k_B T \ln [\Lambda_i^3 \rho_i(z)] + v_i(z) - k_B T c_i^{(1)}(z), \quad (5)$$

where Λ_i is the thermal de Broglie wavelength and $c_i^{(1)}$ is the first-order (single particle) direct correlation function of the ionic species i at z .

This equation shows that the effects of ion-ion interactions on the density profile are wholly contained in $c_i^{(1)}(z)$, which relates to the change in the excess part of the intrinsic free-energy functional of the fluid F^{ex} by^{9,10}

$$c_i^{(1)}(z) = -\beta \frac{\delta F^{\text{ex}}[\rho_i]}{\delta \rho_i(z)}, \quad (6)$$

with $\beta = 1/k_B T$.

Since the chemical potential must be equal everywhere within the system, we can write, for any specific position, say, at the mid-plane $z_m = (h + d)/2$ between the hard walls,

$$\mu_i = k_B T \ln [\Lambda_i^3 \rho_i(z_m)] + v_i(z_m) - k_B T c_i^{(1)}(z_m). \quad (7)$$

This gives, by subtracting Eq. (7) from Eq. (5) together with Eq. (1) for $v_i(z)$,

$$\rho_i(z) = \rho_i(z_m) \exp [c_i^{(1)}(z) - c_i^{(1)}(z_m)], \quad (8)$$

for $d/2 \leq z \leq h + d/2$ and zero otherwise.

Its practical implementation requires, then, a suitable approximation of the first-order direct correlation function. Towards that end, we may decompose $c_i^{(1)}(z)$ into contributions from the Coulomb interaction $c_i^{\text{CO}}(z)$, the hard-sphere exclusions $c_i^{\text{HS}}(z)$, and the cross correlations between these two interactions $c_i^{\text{ES}}(z)$ (i.e., the electric residual contribution⁷),

$$c_i^{(1)}(z) = c_i^{\text{CO}}(z) + c_i^{\text{HS}}(z) + c_i^{\text{ES}}(z) \quad (9)$$

as commonly done by other approaches³⁻¹² of DFT. As a result, Eq. (8) becomes

$$\rho_i(z) = \rho_i(z_m) \exp [-\beta q_i \psi(z) + \Delta c_i^{\text{HS}}(z) + \Delta c_i^{\text{ES}}(z)], \quad (10)$$

with

$$\Delta c_i^{\text{HS}}(z) = c_i^{\text{HS}}(z) - c_i^{\text{HS}}(z_m) \quad (11)$$

and

$$\Delta c_i^{\text{ES}}(z) = c_i^{\text{ES}}(z) - c_i^{\text{ES}}(z_m), \quad (12)$$

where ψ is the mean electrostatic potential, which has been taken to be zero at the mid-plane, and it satisfies the corresponding Poisson equation in one dimension,

$$\psi(z) = \frac{1}{\epsilon_0 \epsilon_r} \sum_i \int_z^{z_m} dz' (z - z') \rho_i(z') q_i, \quad (13)$$

with the electroneutrality condition,

$$\int_0^{(h+d)/2} dz \rho_i(z) q_i + f_i \sigma = 0, \quad (14)$$

where f_i , the fractional surface coverage, is the fraction of surface charge that is compensated by the counterion species i present in the solution.

Since it is well accepted that the fundamental measure theory (FMT)³³ can, as an elegant and powerful approach to DFT for hard spheres, accurately approximate c_i^{HS} , we may use the modified version^{7,34} of FMT to determine $\Delta c_i^{\text{HS}}(z)$ in Eq. (10). The task left is, then, how to provide a reliable estimate of $c_i^{\text{ES}}(z)$, and hence $\Delta c_i^{\text{ES}}(z)$ in Eq. (10), for counterion-only EDLs with the available knowledge³⁻¹² of DFT that have

been successfully used to describe the structural and thermodynamic properties of normal EDLs involving both counter- and co-ions.

A. Approximation of c_i^{ES}

Following the reference-fluid perturbation method³⁻¹² of DFT, a formal “Taylor series” expansion of the non-uniform $c_i^{\text{ES}}(z)$ around a reference fluid with density $\rho_\alpha^{\text{ref}}(z)$ can always be written to give approximately,^{10,35} when it is truncated at the first order,

$$c_i^{\text{ES}}(\mathbf{r}; \rho_i) = c_i^{\text{ES}}(\mathbf{r}; \rho_\alpha^{\text{ref}}) + \sum_\alpha \int d\mathbf{s} (\rho_\alpha(\mathbf{s}) - \rho_\alpha^{\text{ref}}(\mathbf{s})) \times c_{i,\alpha}^{\text{ES}}(\mathbf{r}, \mathbf{s}; \rho_\alpha^*), \quad (15)$$

where for ease of expressing, we have used vectors \mathbf{r} and \mathbf{s} to denote the spatial positions of ions in the system, and run the summation over all kind of ions involved in the reference fluid. $c_{i,\alpha}^{\text{ES}}(\mathbf{r}, \mathbf{s})$ denotes the electric residual contribution to the second-order (pair) direct correlation function. The density field is introduced at the right-hand side of semicolon to clearly specify the fluid in which c_i^{ES} or $c_{i,\alpha}^{\text{ES}}$ is evaluated. In particular, $\rho_\alpha^* = \rho_\alpha^{\text{ref}} + \lambda(\rho_\alpha - \rho_\alpha^{\text{ref}})$ with λ between 0 and 1 represents an intermediate non-uniform density field between ρ_α and ρ_α^{ref} ; as a mixing parameter, λ is generally position dependent, i.e., it is also a function of the coordinate \mathbf{s} for any given ion at position \mathbf{r} .

This equation is actually a functional counterpart of the well-known Lagrangian theorem of differential calculus, and it is exact only if the value of λ is correctly chosen.³⁵ Since in practice it is common to set λ as a constant, independent of both \mathbf{r} and \mathbf{s} , Eq. (15) can only give an approximation of c_i^{ES} . In spite of this, it should be understood that ρ_α^* may be neither ρ_α nor ρ_α^{ref} , and that the definition of ρ_α^* remains somehow flexible.

In addition, it should also be noted that when applied for practical use, almost all DFT approaches³⁻¹² employ the analytical solutions^{13,14} of the first-order and the second-order direct correlation functions from the MSA for homogeneous electrolytes to estimate $c_i^{\text{ES}}(\mathbf{r}; \rho_\alpha^{\text{ref}})$ and $c_{i,\alpha}^{\text{ES}}(\mathbf{r}, \mathbf{s}; \rho_\alpha^*)$, respectively, i.e., to write,

$$c_i^{\text{ES}}(\mathbf{r}; \rho_\alpha^{\text{ref}}) \approx -\beta \mu_i^{\text{ES,MSA}}(\mathbf{r}; \kappa^{\text{ref}}) \quad (16)$$

and

$$c_{i,\alpha}^{\text{ES}}(\mathbf{r}, \mathbf{s}; \rho_\alpha^*) \approx c_{i,\alpha}^{\text{ES,MSA}}(|\mathbf{r} - \mathbf{s}|; \kappa^*), \quad (17)$$

where the superscript MSA refers to the MSA solution, and the inverse of the Debye screening length^{9,10} κ in place of the density field indicates that the MSA solutions depend only on the κ field (the same κ value gives the same results even if the densities are different).

Following the relation between ρ_α^* and ρ_α^{ref} , and the definition of κ (given in the Appendix), we obtain

$$(\kappa^*)^2 = \lambda \kappa^2 + (1 - \lambda)(\kappa^{\text{ref}})^2. \quad (18)$$

This expression will be used later for a suitable choice of the λ value in order to better approximate $c_{i,\alpha}^{\text{ES,MSA}}(|\mathbf{r} - \mathbf{s}|; \kappa^*)$. At the moment, it should be stressed that the use of the MSA solutions implicitly requires that the reference fluid

with density field ρ_α^{ref} should satisfy local charge neutrality, i.e., there must exist some coions, although it does not have to be a physically real fluid.^{5,6} The same principle also applies to the fluid with density field ρ_α^* . As a result, we can drop ρ_α^{ref} from the integrand in Eq. (15) to give

$$c_i^{\text{ES}}(\mathbf{r}; \rho_i) \approx -\beta \mu_i^{\text{ES,MSA}}(\mathbf{r}; \kappa^{\text{ref}}) + \sum_\alpha \int d\mathbf{s} \rho_\alpha(\mathbf{s}) c_{i,\alpha}^{\text{ES,MSA}}(|\mathbf{r} - \mathbf{s}|; \kappa^*). \quad (19)$$

Since no coions are present in our model system, $\rho_\alpha(\mathbf{s}) = 0$ but $\rho_\alpha^{\text{ref}}(\mathbf{s}) \neq 0$ for all kind of coions in the reference fluid. We may go even further to write the above equation as

$$c_i^{\text{ES}}(\mathbf{r}; \rho_i) \approx -\beta \mu_i^{\text{ES,MSA}}(\mathbf{r}; \kappa^{\text{ref}}) + \sum_j \int d\mathbf{s} \rho_j(\mathbf{s}) c_{i,j}^{\text{ES,MSA}}(|\mathbf{r} - \mathbf{s}|; \kappa^*), \quad (20)$$

where we have changed the index of summation from α to j to emphasis the point that the summation only needs to run over all kind of counterions that are present in both the reference fluid and the confined solution in our model system.

This equation essentially states that, although no coions are involved, the first-order direct correlation function $c_i^{\text{ES}}(\mathbf{r})$ of the counterion-only system can still be estimated from the information obtained for counterions from a non-uniform but locally charge-neutral reference fluid. At first glance, it sounds unreasonable. However, the successful applications^{5-7,12} of the RFD and WCA approaches for charged hard-sphere fluids to the cases of EDLs involving dilute electrolytes, where the coions are only marginally present, strongly support that Eq. (20) may be safely used for practical evaluations.

It follows that the accuracy of Eq. (20) is largely dependent on the definition of the reference fluid; the use of different κ^{ref} would give different approximation of $c_i^{\text{ES}}(\mathbf{r}; \rho_i)$. In the cases when one defines several reference fluids, weighting may be applied to the results. That is, to give a better approximation of the first-order direct correlation function, Eq. (20) may be extended by defining a set of reference fluids with different κ^{ref} and setting

$$\mu_i^{\text{ES,MSA}}(\mathbf{r}; \kappa^{\text{ref}}) = \sum_m \gamma_m \mu_i^{\text{ES,MSA}}(\mathbf{r}; \kappa_m^{\text{ref}}) \quad (21)$$

and

$$c_{i,j}^{\text{ES,MSA}}(|\mathbf{r} - \mathbf{s}|; \kappa^*) = \sum_m \gamma_m c_{i,j}^{\text{ES,MSA}}(|\mathbf{r} - \mathbf{s}|; \kappa_m^*), \quad (22)$$

where the weighting factors fulfill the normalized conditions, i.e.,

$$\sum_m \gamma_m = 1. \quad (23)$$

The key problem is, then, how to define κ_m^{ref} properly and to give a good approximation of $c_{i,j}^{\text{ES,MSA}}(|\mathbf{r} - \mathbf{s}|; \kappa_m^*)$ with a suitable choice of the mixing parameters of λ_m , especially in the case of $m = 1$.

B. Construction of κ^{ref}

To facilitate the evaluation of $\mu_i^{\text{ES,MSA}}(\mathbf{r}; \kappa^{\text{ref}})$, we may construct the reference fluid in such a way that it is not only

charge neutral but also has the same κ value at every location z as that given by ρ_i of the model system, i.e., to define

$$\kappa^{\text{ref}}(z) = \kappa(z). \quad (24)$$

This reference fluid has actually been used (but not explicitly stated) in the WCA approach, developed by Wang *et al.*,⁷ for evaluation of the weighted correlation functions. We may, therefore, refer to it as the κ^{WCA} reference fluid.

Alternatively, the idea of Gillespie *et al.*⁵ can be followed to give

$$\kappa^{\text{ref}}(z) = \int dz' \kappa^{\text{WCA}}(z') w^{\text{RFD}}(z, z'), \quad (25)$$

with the weight function,

$$w^{\text{RFD}}(z, z') = \frac{3}{4\pi} \frac{\Theta(|z' - z| - R_{\text{filter}}(z))}{R_{\text{filter}}^3(z)}, \quad (26)$$

where we have used the superscript RFD to highlight the fact that this weight function is actually the one proposed by Gillespie *et al.*⁵ in developing their RFD approach to DFT, and Θ is the unit step function: $\Theta(z) = 1$ for $z \leq 0$ and $\Theta(z) = 0$ for $z > 0$.

In this equation, the capacitance radius R_{filter} defines the spherical volume over which κ^{WCA} is averaged, and for the restricted primitive model (RPM), it simplifies from its general definition⁵ to

$$R_{\text{filter}}(z) = \frac{d}{2} + \frac{1}{2\Gamma^{\text{ref}}(z)}, \quad (27)$$

where $\Gamma^{\text{ref}}(z)$ is the MSA inverse screening length, which can readily be determined from κ^{ref} (see the Appendix for details).

The fluid thus constructed through Eqs. (25)–(27) may be named κ^{RFD} reference fluid due to the use of $w^{\text{RFD}}(z, z')$, as given in Eq. (26).

A more complicated reference fluid can even be proposed, by, e.g., averaging κ^{RFD} with a weight function similar to that suggested by Denton and Ascroft³⁶ in developing a WDA approach to DFT, i.e., to define

$$\kappa^{\text{ref}}(z) = \int dz' \kappa^{\text{RFD}}(z') w^{\text{WDA}}(z, z'), \quad (28)$$

with the weight function given by

$$w^{\text{WDA}}(z, z') = \frac{C_{00}^{\text{ES,MSA}}(|z' - z|, \kappa^{\text{ref}}(z))}{\int_{z-d}^{z+d} dz' C_{00}^{\text{ES,MSA}}(|z' - z|, \kappa^{\text{ref}}(z))}, \quad (29)$$

where we have used the superscript WDA to emphasis that this weight function is one inspired by the work of Denton and Ascroft,³⁶ and given the expression of the $C_{00}^{\text{ES,MSA}}$ function in the Appendix. The result may be referred to as the κ^{WDA} reference fluid.

Although it might be worth to discuss in detail the effects of different choice of κ^{ref} on the approximation of $c_i^{\text{ES}}(\mathbf{r}; \rho_i)$, we do not work on this in the current study but use the κ^{WDA} reference fluid to evaluate $\mu_i^{\text{ES,MSA}}(\mathbf{r}; \kappa^{\text{ref}})$ as a starting point, i.e., to set

$$\kappa^{\text{ref}}(z) = \kappa^{\text{WDA}}(z) \quad (30)$$

and subsequently,

$$\mu_i^{\text{ES,MSA}}(\mathbf{r}; \kappa^{\text{ref}}) = \mu_i^{\text{ES,MSA}}(\kappa) \Big|_{\kappa=\kappa^{\text{WDA}}(\mathbf{r})}, \quad (31)$$

where we have highlighted the explicit dependence of the $\mu_i^{\text{ES,MSA}}$ solution on κ .

We use, however, both κ^{RFD} and κ^{WCA} reference fluids to approximate $c_{i,j}^{\text{ES,MSA}}(|\mathbf{r}-\mathbf{s}|; \kappa^*)$ in Eq. (20), as detailed in what follows.

C. Approximation of $c_{i,j}^{\text{ES}}$

As discussed above, the mixing parameter λ is dependent on coordinates \mathbf{r} and \mathbf{s} . When used in practice,^{3–12} however, it is common to define λ as a constant. If $\lambda = 0$ is set, κ^* would simply be reduced to κ^{ref} , as seen from Eq. (18). Even in this case, there is enough flexibility in the estimation of $c_{i,j}^{\text{ES,MSA}}(|\mathbf{r}-\mathbf{s}|; \kappa^*)$. For instance, in the case of using κ^{RFD} to construct the reference fluid, one can use the κ^{RFD} value at the middle position \mathbf{m} between \mathbf{r} and \mathbf{s} to give

$$c_{i,j}^{\text{ES,MSA}}(|\mathbf{r}-\mathbf{s}|; \kappa^*) = c_{i,j}^{\text{ES,MSA}}(|\mathbf{r}-\mathbf{s}|; \kappa) \Big|_{\kappa=\kappa^{\text{RFD}}(\mathbf{m})}. \quad (32)$$

If $\lambda = 1$ is chosen instead, κ^* would become κ or equivalently κ^{WCA} from Eq. (18), and therefore one can write

$$c_{i,j}^{\text{ES,MSA}}(|\mathbf{r}-\mathbf{s}|; \kappa^*) = c_{i,j}^{\text{ES,MSA}}(|\mathbf{r}-\mathbf{s}|; \kappa) \Big|_{\kappa=\kappa^{\text{WCA}}(\mathbf{m})}. \quad (33)$$

This kind of evaluations satisfy the symmetry condition of the second-order direct correlation function, but use only the properties of one homogenous fluid corresponding to either $\kappa^{\text{RFD}}(\mathbf{m})$ or $\kappa^{\text{WCA}}(\mathbf{m})$ to estimate the ion-ion correlations in an inhomogeneous fluid. As a result, it works well solely in the limiting case of weakly coupled systems where multivalent counterions are absent. Partly for this reason, and partly for an attempt to keep the structural and the thermodynamic properties of the EDLs self-consistent, we do not use Eqs. (32) and (33) in this study but make a “Taylor series” expansion of $c_{i,j}^{\text{ES,MSA}}(|\mathbf{r}-\mathbf{s}|; \kappa^*(\mathbf{m}))$ around $\kappa^{\text{RFD}}(\mathbf{m})$ and $\kappa^{\text{WCA}}(\mathbf{m})$, respectively. This gives, when the series are truncated at the first order with a constant λ value and Eq. (18) is used,

$$c_{i,j}^{\text{ES,MSA}}(|\mathbf{r}-\mathbf{s}|; \kappa^*) \approx \lambda c_{i,j}^{\text{ES,MSA}}(|\mathbf{r}-\mathbf{s}|; \kappa) \Big|_{\kappa=\kappa^{\text{WCA}}(\mathbf{m})} + (1-\lambda) c_{i,j}^{\text{ES,MSA}}(|\mathbf{r}-\mathbf{s}|; \kappa) \Big|_{\kappa=\kappa^{\text{RFD}}(\mathbf{m})}. \quad (34)$$

The functioning of λ changes now from mixing the densities to mixing the second-order direct correlation functions. In this manner, Eq. (34) is actually equivalent to Eq. (22) with $m = 2$, and it is also the result of the binomial version of the WCA approach.^{7,8}

It should, however, be noted that Eq. (34) is obtained on the basis of Eq. (18) with the definition of $\kappa^{\text{ref}} = \kappa^{\text{RFD}}$, and therefore κ^{RFD} should be used to evaluate $\mu_i^{\text{ES,MSA}}(\mathbf{r}; \kappa^{\text{ref}})$ in Eq. (20). Nevertheless, we find that the replacement of κ^{RFD} with κ^{WDA} , as given in Eq. (31), gives a slightly better description of the interfacial properties of EDLs. The reason for this is not clear yet, but it suggests that the use of κ^{WDA} reference fluid decreases the truncation error associated with Eq. (34). As a result, in this study, we use Eqs. (31) and (34) together to approximate $c_i^{\text{ES}}(\mathbf{r}; \rho_i)$ in Eq. (20).

D. Determination of λ

When Eqs. (31) and (34) are used in Eq. (20) to evaluate $c_i^{\text{ES}}(\mathbf{r}; \rho_i)$, we find from Eq. (10) that

$$\ln \rho_i(z, \lambda) = \lambda \ln \rho_i(z, \lambda)|_{\lambda=1} + (1-\lambda) \ln \rho_i(z, \lambda)|_{\lambda=0}, \quad (35)$$

where we have made the dependence of the calculated $\rho_i(z)$ profile on λ explicit and use $\rho_i(z, \lambda)|_{\lambda=0}$ and $\rho_i(z, \lambda)|_{\lambda=1}$ to specify the density profiles calculated when we select $\lambda = 0$ and 1, corresponding to the use of Eqs. (32) and (33) for approximation of $c_{i,j}^{\text{ES,MSA}}(|\mathbf{r}-\mathbf{s}|; \kappa^*)$, respectively.

Alternatively, the linearized version of Eq. (10) or Eq. (35) allows us to write

$$\rho_i(z, \lambda) \approx \lambda \rho_i(z, \lambda)|_{\lambda=1} + (1-\lambda) \rho_i(z, \lambda)|_{\lambda=0}. \quad (36)$$

This expression states that the density profile at equilibrium can be approximated as a weighted sum of the density profiles calculated with $\lambda = 0$ and 1, respectively. In practice, it was found that both Eqs. (35) and (36) work equally well in describing the structures of the counterion-only EDLs. The key point that matters is the suitable setting of λ . To address this problem, we noticed that combination of Eqs. (4) and (36) gives rise to

$$P(h, \lambda) = \lambda P(h, \lambda)|_{\lambda=1} + (1-\lambda) P(h, \lambda)|_{\lambda=0}. \quad (37)$$

This result may be used for determination of the mixing parameter λ by following the approach of Zhou³⁵ on the reasoning that λ is, as an approximation, independent of the separation h . That is, for a specific case of σ and f_i , the calculated density profile should be enforced to fulfill the exact contact theorem in the limiting case as $h \rightarrow \infty$, or in other words,

$$\lim_{h \rightarrow \infty} P(h, \lambda) = \lim_{h \rightarrow \infty} P_{\text{exp}}(h), \quad (38)$$

where P_{exp} is the “real” pressure of the confined solution, whereas P is the “calculated” pressure from Eq. (4).

Since for counterion-only EDLs P_{exp} goes to zero as $h \rightarrow \infty$, the above two equations yield

$$\lambda = \lim_{h \rightarrow \infty} \frac{P(h, \lambda)|_{\lambda=0}}{P(h, \lambda)|_{\lambda=0} - P(h, \lambda)|_{\lambda=1}}. \quad (39)$$

The λ value can, therefore, be determined from the case where h has been set to be large enough, at which the calculated pressure $P(h, \lambda)|_{\lambda=1}$ has become negative while $P(h, \lambda)|_{\lambda=0}$ remains positive when divalent counterions are involved (one can simply set $\lambda = 0$ for the monovalent counterion-only systems). Once it was obtained, we may proceed to the cases of small separations of planar charged walls.

With this approach, it is anticipated that the structural and thermodynamic properties of EDLs would be kept consistence due to the use of the MSA solutions of the first-order and the second-order direct correlation functions and also Eq. (38), which make both the density profile and the pressure being correctly predicted at least in the large h cases.

To summarize, the self-consistent WCA approach uses FMT to evaluate $c_i^{\text{HS}}(z)$ and Eq. (20) to approximate $c_i^{\text{ES}}(z)$, respectively, to implement Eq. (10) for the $\rho_i(z)$ profile of the counterion-only EDL at equilibrium. This requires the definition of $\kappa^{\text{WCA}}(z)$ via Eq. (24), $\kappa^{\text{RFD}}(z)$ via Eqs. (25)–(27),

and $\kappa^{\text{WDA}}(z)$ via Eqs. (28) and (29), and subsequently the evaluation of $\mu_i^{\text{ES,MSA}}(z; \kappa^{\text{ref}})$ by Eq. (31) as well as $c_{i,j}^{\text{ES,MSA}}(|\mathbf{r} - \mathbf{s}|; \kappa^*)$ by Eq. (34), with the help of Eqs. (32) and (33). The λ value used to mix the density profiles in Eq. (36) is to be determined from Eq. (39). Whenever necessary, we use Eq. (4) to calculate the pressure of the confined solution between two planar charged walls.

IV. RESULTS AND DISCUSSION

The nonlinear integral equation for density profiles at equilibrium, i.e., Eq. (10), is solved using the Picard iteration method, with the modified Gouy-Chapman result¹⁵ for counterion-only EDLs as an initial guess, for several values of the surface charge density σ . Since our interest is mainly on exploring the capability of the self-consistent WCA approach in evaluating the swelling behavior of montmorillonite, the main component of natural bentonite, we restrict σ to be in the range between -0.05 and -0.13 C m^{-2} .³⁸ The other parameter values used in our calculations correspond to those of the RPM simulations by Segad *et al.*,³⁷ in order to validate our MC algorithms and are given here as $d = 4.0 \text{ \AA}$, $T = 298.0 \text{ K}$, and $\varepsilon_r = 78.0$.

Before proceeding, we present in Fig. 1 the density profiles for the system with $\sigma = -0.11 \text{ C m}^{-2}$ at surface separations $h = 3, 5, 8$, and 10 \AA , respectively, where the results from the MC simulations and the self-consistent WCA calculations are

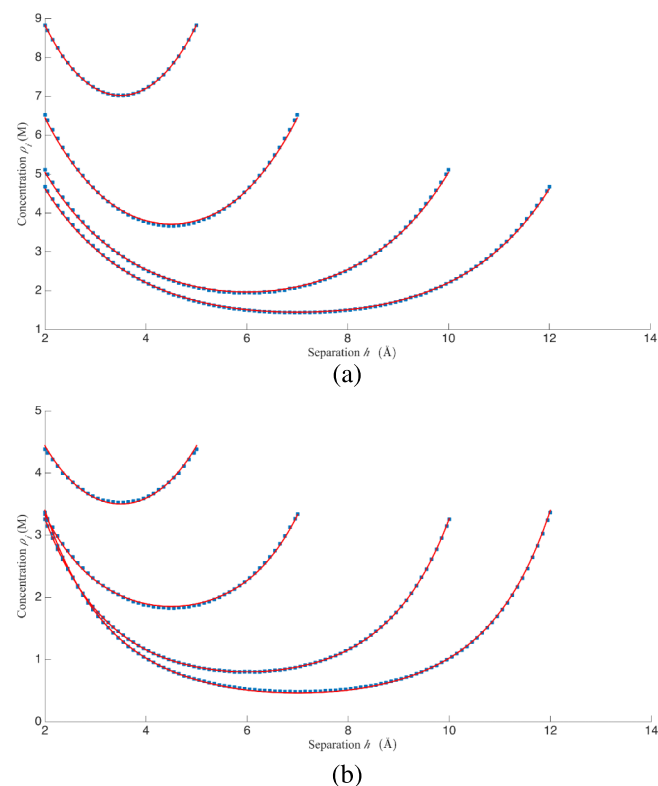


FIG. 1. Density profiles in mol dm^{-3} for (a) monovalent counterions and (b) divalent counterions between two planar charged walls ($\sigma = -0.11 \text{ C m}^{-2}$) for surface separations $h = 3, 5, 8$, and 10 \AA , respectively. The solid squares show the results from MC simulations and the curves are from the self-consistent WCA calculations.

compared. It is seen that the MC and WCA values agree very well with each other in both cases when the surface charges are compensated by either mono- or divalent counterions. The density profiles are all parabolic in shape, and no qualitative difference from the results of the Gouy-Chapman theory^{15,16} can be found.

Note, however, that we simply set $\lambda = 0$ in the case involving only monovalent counterions. This setting reduces the self-consistent WCA approach to the RFD approach, showing its robustness in accounting for the cross correlations between the Coulombic interaction and the hard-sphere exclusion. In the case involving only divalent counterions, however, the λ value determined from Eq. (39) was found to be around 0.5, indicating the necessity to apply Eq. (33), the WCA approximation to $c_{i,j}^{\text{ES,MSA}}(|\mathbf{r} - \mathbf{s}|; \kappa^*)$, to accommodate that of the RFD approach in Eq. (34) in order to give an accurate account of the coupling effect of the electrostatic-excluded volume correlations.

Following this, we shall now focus on discussion of the pressures under different conditions (since our objective is to show the agreement between the results of the proposed approach and the MC simulations, we do not particularly work on the total pressure, which also includes the contribution of the van der Waals interaction and has been well studied by Segad *et al.*³⁷). In Fig. 2, the pressures for a system with mono- or divalent counterions are shown for several values of the surface charge density. The agreement between the MC and the self-consistent WCA results is seen to be excellent for all separations calculated. In addition, we find that monovalent

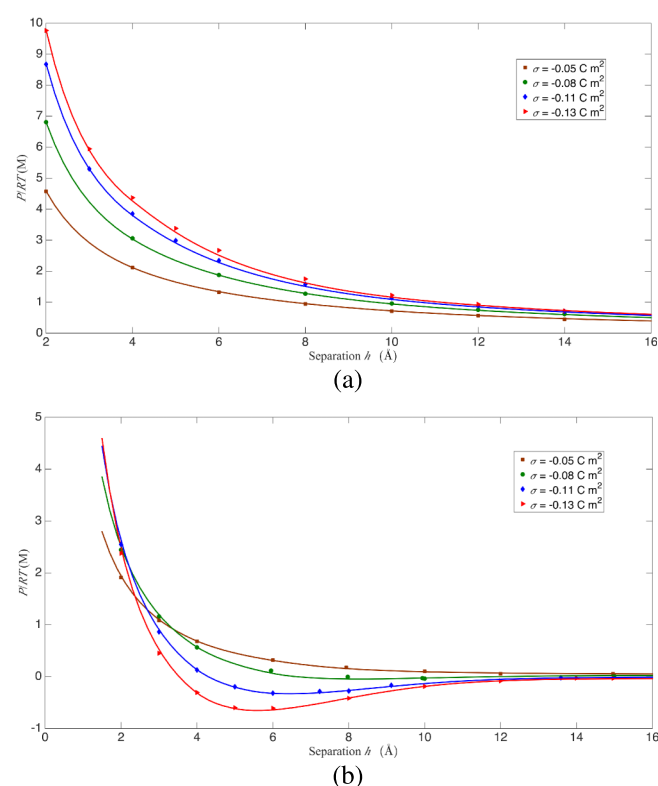


FIG. 2. The pressure between two planar charged walls as a function of separation for a system with (a) monovalent counterions and (b) divalent counterions, respectively. The solid markers show the results from MC simulations and the curves are from the self-consistent WCA calculations. The surface charge density is indicated in the figure.

counterions always lead to a monotonic repulsion between two planar charged walls. This result is consistent with the experimental observations^{24,25} that the purified and fully Na-exchanged bentonite always expanded in distilled water in a vertical test tube until the entire volume of the tube was fully occupied by colloidal particles. It explains, at least partly, why the DLVO theory²³ can be used successfully to predict the swelling and erosion behavior of Na-bentonite in distilled water or dilute solutions.^{22–25}

With divalent counterions, however, the pressures show complete different characteristics; a negative shallow minimum is observed at a separation distance of ~ 0.6 nm when $\sigma \leq -0.08$ C m⁻². As a sign of attraction, resulting from ion-ion correlations, this shallow minimum deepens and its position shifts to small values of separation with an increase in surface charge density.

Of great importance is, nevertheless, to see that the MC and WCA results still agree nicely with each other, showing excellent ability of the self-consistent WCA approach in describing the thermodynamic properties of counterion-only EDLs even when electrostatic correlation effects become relatively important in comparison to those of ionic excluded volume and direct Coulomb interactions. The corresponding pressures calculated with the Poisson-Boltzmann equation or the modified Gouy-Chapman theory are, however, not shown in Fig. 2 for comparison, because these approaches have long been studied and shown to give a qualitatively correct result for the cases involving monovalent counterions but incorrect result for the cases involving divalent counterions.^{37,39}

It follows that the self-consistent WCA approach also works well in the case involving both mono- and divalent counterions, as shown in Fig. 3 for a system with $\sigma = -0.11$ C m⁻². Clearly, the more divalent counterions such as Ca²⁺ in the solution are exchanged for monovalent counterions, say Na⁺, the more the system behaves like that involving only monovalent counterions. This is especially true when the fraction of surface charge compensated by monovalent counterions, i.e., f_{Na} , is greater than 30%. Only below this critical fraction can a shallow minimum be observed on the curve of the pressure vs. separation, which deepens and the position shifts to small values of separation with a decrease in f_{Na} . This result is, in

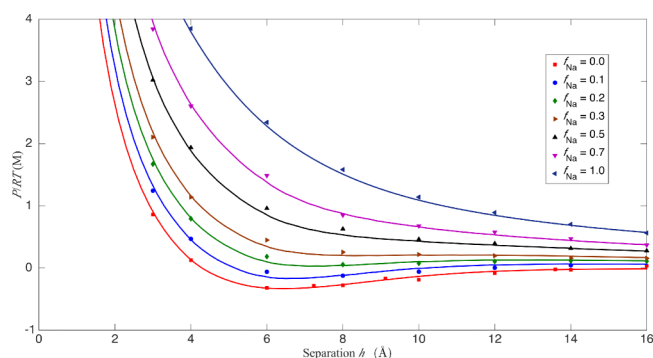


FIG. 3. The pressure between two planar charged walls ($\sigma = -0.11$ C m⁻²) as a function of separation for a system involving both mono- and divalent counterions. The solid markers show the results from MC simulations and the curves are from the self-consistent WCA calculations. The fraction of surface charge compensated by monovalent counterions in the solution is indicated in the figure.

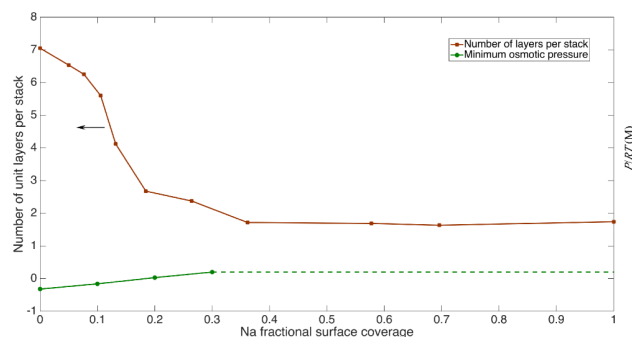


FIG. 4. The number of clay plates (unit layers of montmorillonite) per stack as a function of surface coverage for exchange of Ca²⁺ with Na⁺ in a salt-free system.²⁶ The value of the shallow minimum of the pressure curve in Fig. 3 calculated from the self-consistent WCA approach is also shown in the figure. The dashed line indicates the region where no shallow minimum was observed on the curve of the pressure vs. separation.

essence, consistent with the experimental findings²⁶ that upon exchange of Ca-counterions for Na-counterions, a sharp initial decrease in the size of stacks (tactoids) of dilute suspensions of montmorillonites was observed over roughly the first 30% of fractional surface coverage of Na⁺, as shown in Fig. 4. Upon further exchange, stack sizes changed only slightly.

In Fig. 4, the values of the shallow minimum of the pressure curves in Fig. 3 calculated from the self-consistent WCA approach are also shown for the cases of $f_{\text{Na}} \leq 30\%$. It is seen that an enhanced attraction between the clay particles, with less monovalent counterions, leads to a large size of the stacks of montmorillonite. The stack sizes reduced from seven layers at $f_{\text{Na}} = 0\%$ to one to two layers at $f_{\text{Na}} = 30\%$, and changed slightly with further increase in f_{Na} when the pressure has become a monotonically decreasing function of separation. This close correlation between the number of clay plates per stack and the value of the shallow minimum of the pressure curve explains the reason for the stack formation in montmorillonite in aqueous systems of Ca-dominated bentonites.²² It gives, however, no clear insight into the mechanisms that make the purified and fully Ca-exchanged bentonite (initially compacted) swelling in distilled water more rapidly than Na-bentonites in the beginning but stopped expansion when its volume was increased to roughly four times in a vertical test tube.^{24,25} The breakup of montmorillonite stacks into small particles due to osmotic swelling²² also cannot be addressed by the RPM of counterion-only EDLs. A more realistic model of the clay system is, therefore, expected to account for the effects of, e.g., the structuring of solvent molecules, the heterogeneous distribution of surface charges, and the hetero-interaction between stacks of montmorillonite on the pressure and subsequently on the stability of colloidal clay in salt-free or dilute solutions.

V. SUMMARY AND CONCLUSIONS

Based on the functional counterpart of the Lagrangian theorem of differential calculus, i.e., Eq. (15), a self-consistent WCA approach to DFT is developed in this study. It utilizes the analytical solutions of the first-order and the second-order direct correlation functions from the MSA for a homogeneous

electrolyte to define a reference fluid and to account for the coupling effect of the electrostatic-excluded volume correlations in the RPM of counterion-only EDLs. The λ parameter introduced in the approach is used to mix the evaluations of $c_{i,j}^{\text{ES,MSA}}(|\mathbf{r}-\mathbf{s}|; \kappa^*)$ in Eq. (34), and also to weight the density profiles at equilibrium in Eq. (36), from the application of both the κ^{WCA} and κ^{RFD} reference fluids. It is to be determined by Eq. (39), by requiring that the calculated density profile fulfills the exact contact theorem in the limiting case as $h \rightarrow \infty$.

When applied for evaluating the homo-interaction between clay particles in salt-free solutions, it is found that the MC and WCA results agree excellently with each other in the cases of practical interest, with $\sigma = -0.05$ to -0.13 C m $^{-2}$ involving both mono- and divalent counterions. This verification clearly demonstrates the reliability and robustness of the self-consistent WCA approach in describing the cross correlations between the Coulombic interaction and the hard-sphere exclusion.

More importantly, the study shows that the relative importance of electrostatic correlations in comparison to the effects of ionic excluded volume and direct Coulomb interactions depends on the valency of the counterions and the surface charge density. In a system with mixed counterions, e.g., Na $^{+}$ and Ca $^{2+}$, the competition between the ions makes the clay always swelling in a way much like purified and fully Na-exchanged bentonites²²⁻²⁵ when the fraction of surface charge compensated by monovalent counterions f_{Na} is greater than 30%. The larger the Na fractional surface coverage is, the stronger the monotonic repulsion between the clay particles becomes. In the opposite situation when Ca $^{2+}$ dominates with $f_{\text{Na}} < 30\%$, a shallow minimum is always present on the pressure curve leading to an attraction that favors the formation of stacks in the clay system. The less the Na fractional surface coverage is, the more clay plates the stack contains, making Ca-dominated bentonites very limited in swelling. In a clay system with only divalent counterions, a surface charge density around -0.08 C m $^{-2}$ (not accounting for the van der Waals interaction) is sufficient to aggregate the clay particles in a face-to-face orientation into stacks incorporating a water layer of ~ 1.0 nm.

Although these findings, from both the MC simulations and the WCA calculations, are consistent with some of the experimental observations,²⁴⁻²⁶ they cannot be used to explain the swelling behavior of purified and fully Ca-exchanged bentonite, and the breakup of clay stacks into small particles during the process of osmotic swelling.^{22,27} It is anticipated that a more realistic model than the RPM might give more insights into the mechanisms governing the stability of colloidal clay in salt-free or dilute solutions, by accounting for the effects of, e.g., the structuring of solvent molecules, the heterogeneous distribution of surface charges, and the hetero-interaction between clay stacks.

In addition, it might be interesting to show the effects of various radii of ions on the pressure in different cases, and following the approach of Wang *et al.*⁴⁰ or Kjellander *et al.*²⁰ to analyze the kinetic, the electrostatic-correlation, and the hard-core contributions to the pressure in detail. Last but not least, it should be emphasized that the idea behind the self-consistent WCA approach can readily be extended to formulate a novel DFT approach that may give a faithful description of

the structural and thermodynamic properties of normal EDLs in equilibrium with a salt reservoir. These will be done in the near future.

ACKNOWLEDGMENTS

The author gratefully acknowledges the encouragement and financial support of the Swedish Nuclear Fuel and Waste Management Company (SKB). The work was also partly funded by the European Union through the BELBaR project. In particular, expressions of sincere gratitude are given to Professor Ivars Neretnieks for fruitful discussions on the theory development and the predicted results.

APPENDIX: THE MSA SOLUTIONS OF A HOMOGENEOUS FLUID

Several MSA solutions to the properties of the RPM of a homogeneous fluid have been used in discussing the self-consistent WCA approach to DFT, which are described here.

1. The first-order direct correlation function

For a homogeneous ionic hard-sphere fluid, the first-order direct correlation function c_i^{ES} is position-independent and it simply relates to the electrostatic component μ_i^{ES} of the excess chemical potential by

$$c_i^{\text{ES}} = -\beta\mu_i^{\text{ES}}. \quad (\text{A1})$$

With the general MSA solution¹⁴ but applied to the RPM case, we can write

$$\mu_i^{\text{ES,MSA}} = -\frac{q_i^2}{4\pi\epsilon_0\epsilon_r} \frac{\Gamma}{1+\Gamma d}, \quad (\text{A2})$$

where Γ , the MSA inverse screening length, is determined by

$$\kappa = 2\Gamma(1+\Gamma d), \quad (\text{A3})$$

with κ , the inverse of the Debye screening length, defined as

$$\kappa^2 = \frac{\beta}{\epsilon_0\epsilon_r} \sum_i \rho_i q_i^2. \quad (\text{A4})$$

2. The second-order direct correlation function

Following the MSA solution of Waisman and Lebowitz,¹³ the electric residual contribution to the second-order direct correlation function can be written as

$$c_{i,j}^{\text{ES,MSA}}(r) = \frac{\beta q_i q_j}{4\pi\epsilon_0\epsilon_r r} \left(1 - \frac{\Gamma r}{1+\Gamma d}\right)^2 \Theta(r-d). \quad (\text{A5})$$

When used in the approximation of $c_{i,j}^{\text{ES}}(\mathbf{r}, \mathbf{s})$ for an inhomogeneous fluid with the density field depending only on z , an integration of the form¹¹

$$C_{i,j}^{\text{ES,MSA}}(z) = 2\pi \int_z^\infty ds c_{i,j}^{\text{ES,MSA}}(s)s \quad (\text{A6})$$

is often used, and it can explicitly be written as

$$C_{i,j}^{\text{ES,MSA}}(z) = \frac{\beta q_i q_j}{2\epsilon_0\epsilon_r} C_{00}^{\text{ES,MSA}}(z, \kappa), \quad (\text{A7})$$

with the $C_{00}^{\text{ES,MSA}}(z, \kappa)$ function given by

$$C_{00}^{\text{ES,MSA}}(z, \kappa) = d \left[\frac{B^2}{3} \left(1 - \frac{z^3}{d^3} \right) - B \left(1 - \frac{z^2}{d^2} \right) + \left(1 - \frac{z}{d} \right) \right] \times \Theta(z - d), \quad (\text{A8})$$

where the B parameter is an implicit function of κ , and it is related to Γ by

$$B = \frac{\Gamma d}{1 + \Gamma d}. \quad (\text{A9})$$

Thus, as a factor of $C_{i,j}^{\text{ES,MSA}}(z)$, $C_{00}^{\text{ES,MSA}}(z, \kappa)$ contains no information about the Coulombic interactions between ions i and j , but only a function of the property of the homogeneous fluid, i.e., κ , and the separation distance z . It is this function that has been used in defining the κ^{WDA} reference fluid, as described in Eqs. (28) and (29). Although the result would not differ if one replaces $C_{00}^{\text{ES,MSA}}(z, \kappa)$ by $C_{i,j}^{\text{ES,MSA}}(z)$ in Eq. (29), the notation of $C_{00}^{\text{ES,MSA}}(z, \kappa)$ makes it clear that $w^{\text{WDA}}(z, z')$ is q_i and q_j charge-independent.

¹R. Evans and T. J. Sluckin, *Mol. Phys.* **40**, 413 (1980).

²M. M. Telo Da Gama, R. Evans, and T. J. Sluckin, *Mol. Phys.* **41**, 1355 (1980).

³Z. Tang, L. E. Scriven, and H. T. Davis, *J. Chem. Phys.* **97**, 9258 (1992).

⁴C. N. Patra and S. K. Ghosh, *J. Chem. Phys.* **117**, 8938 (2002).

⁵D. Gillespie, W. Nonner, and R. S. Eisenberg, *Phys. Rev. E* **68**, 031503 (2003).

⁶M. G. Knepley, D. A. Karpeev, S. Davidovits, R. S. Eisenberg, and D. Gillespie, *J. Chem. Phys.* **132**, 124101 (2010).

⁷Z. Wang, L. Liu, and I. Neretnieks, *J. Phys.: Condens. Matter* **23**, 175002 (2011).

⁸Z. Wang and L. Liu, *Phys. Rev. E* **86**, 031115 (2012).

⁹P. Attard, *Thermodynamics and Statistical Mechanics: Equilibrium by Entropy Maximization* (Academic, London, 2002).

¹⁰J.-P. Hansen and I. R. McDonald, *Theory of Simple Fluid* (Academic, London/New York, 2006).

¹¹S. L. Carnie, D. Y. C. Chan, D. J. Mitchell, and B. W. Ninham, *J. Chem. Phys.* **74**, 1472 (1981).

¹²J. Jiang, D. Cao, D. Henderson, and J. Wu, *J. Chem. Phys.* **140**, 044714 (2014).

¹³E. Waisman and J. L. Lebowitz, *J. Chem. Phys.* **56**, 3093 (1972).

¹⁴W. Nonner, D. Gillespie, D. Henderson, and B. Eisenberg, *J. Phys. Chem. B* **105**, 6427 (2001).

¹⁵D. F. Evans and H. Wennerström, *The Colloidal Domain: Where Physics, Chemistry, Biology, and Technology Meet*, 2nd ed. (Wiley-VCH, New York, 1999).

¹⁶D. Henderson, *Prog. Surf. Sci.* **13**, 197 (1983).

¹⁷J. A. Greathouse, S. E. Feller, and D. A. McQuarrie, *Langmuir* **10**, 2125 (1994).

¹⁸A. G. Moreira and R. R. Netz, *Europhys. Lett.* **52**, 705 (2000).

¹⁹W. H. Briscoe and P. Attard, *J. Chem. Phys.* **117**, 5452 (2002).

²⁰R. Kjellander, T. Åkesson, B. Jönsson, and S. Marelja, *J. Chem. Phys.* **97**, 1424 (1992).

²¹H. Greberg and R. Kjellander, *Mol. Phys.* **87**, 407 (1996).

²²L. Liu, *Colloids Surf., A: Physicochem. Eng. Aspects* **434**, 303 (2013).

²³L. Liu, L. Moreno, and I. Neretnieks, *Langmuir* **25**, 679 (2009).

²⁴L. Liu, *Colloids Surf., A: Physicochem. Eng. Aspects* **358**, 68 (2010).

²⁵L. Liu, I. Neretnieks, and L. Moreno, *Phys. Chem. Earth* **36**, 1783 (2011).

²⁶L. L. Schramm and J. C. T. Kwak, *Clays Clay Miner.* **30**, 40 (1982).

²⁷O. Karnland, S. Olsson, and U. Nilsson, "Mineralogy and sealing properties of various bentonite and smectite-rich clay materials," SKB Technical Report TR-06-30 (Swedish Nuclear Fuel and Waste Management Co., Stockholm, Sweden, 2006).

²⁸L. Liu, L. Moreno, and I. Neretnieks, *Langmuir* **25**, 688 (2009).

²⁹S. Lamperski, *Mol. Simul.* **33**, 1193 (2007).

³⁰N. Metropolis, A. W. Rosenbluth, M. N. Rosenbluth, A. H. Teller, and E. Teller, *J. Chem. Phys.* **21**, 1087 (1953).

³¹D. Boda, K.-Y. Chan, and D. Henderson, *J. Chem. Phys.* **109**, 7362 (1998).

³²M. Bester and V. Vlady, *J. Chem. Phys.* **96**, 7656 (1992).

³³R. Roth, *J. Phys.: Condens. Matter* **22**, 063102 (2010).

³⁴Y.-X. Yu and J. Wu, *J. Chem. Phys.* **117**, 10156 (2002).

³⁵S. Zhou, *New J. Phys.* **4**, 36 (2002).

³⁶A. R. Denton and N. W. Ashcroft, *Phys. Rev. A* **44**, 8242 (1991).

³⁷M. Segad, B. Jönsson, T. Åkesson, and B. Cabane, *Langmuir* **26**, 5782 (2010).

³⁸G. Lagaly, "Colloid clay science," in *Handbook of Clay Science, Developments in Clay Science*, edited by F. Bergaya, B. K. G. Theng, and G. Lagaly (Elsevier, Amsterdam, Netherlands, 2006), Vol. 1.

³⁹R. Kjellander and S. Marčelja, *Chem. Phys. Lett.* **127**, 402 (1986).

⁴⁰Z. Wang, L. Liu, and I. Neretnieks, *J. Chem. Phys.* **135**, 244107 (2011).